Dynamical Fragment Production as a Mode of Energy Dissipation in Heavy-Ion Reactions

J. Tõke, D. K. Agnihotri, S. P. Baldwin, B. Djerroud, B. Lott,* B. M. Quednau,* W. Skulski, and W. U. Schröder
Department of Chemistry and Nuclear Structure Research Laboratory, University of Rochester, Rochester, New York 14627

L. G. Sobotka, R. J. Charity, and D. G. Sarantites
Department of Chemistry, Washington University, St. Louis, Missouri 63130

R. T. de Souza
Department of Chemistry and Indiana University Cyclotron Facility, Indiana University, Bloomington, Indiana 47405
(Received 15 March 1996)

Based on measured correlations between experimental observables in the ^{209}Bi + ^{136}Xe reaction at $E/A = 28$ MeV, it is shown that multiple intermediate-mass fragment (IMF) production is a dynamical process driven by the energy of relative motion of projectilelike and targetlike fragments. This kinetic energy is converted into thermal energy of the system, until a certain "saturation" value of approximately 3 MeV/nucleon is reached. From this point on, this "conventional" dissipation mechanism is replaced by dynamical IMF production, constituting a new mode of energy dissipation. [S0031-9007(96)01493-7]

PACS numbers: 25.70.Lm, 25.70.Mn, 25.70.Pq

Over the last decade, one of the central issues driving intermediate-energy heavy-ion reaction studies has been a phenomenon termed "multifragmentation" [1–4] whose experimental signature is the presence of multiple intermediate-mass fragments (IMF) in the reaction exit channel. Since the observed IMF multiplicities are significantly higher than can be explained by standard statistical-model calculations, various models and scenarios have been considered in the past [5–9] which favor copious production of IMFs. The present paper shows that the current models cannot be reconciled with all of the fundamental experimental observations. Based on a set of fundamental observations, a new scenario for intermediate-energy heavy-ion reactions is proposed which connects in a natural way the domain of dissipative collisions [10] with that of multiple IMF production.

The experiment was performed at the National Superconducting Cyclotron Laboratory of Michigan State University and provided for a measurement of both charged products and neutrons from the ^{209}Bi + ^{136}Xe reaction at $E/A = 28$ MeV, with virtually 4π angular coverage. A detailed account of the experimental procedures is given elsewhere [11–14]. The present paper discusses data on IMFs ($Z \geq 3$), neutrons, and projectilelike fragments (PLF, with $10 \leq Z_{\mathrm{PLF}} \leq 54$), obtained with the Washington University Dwarf array [15], the Rochester University 900 liter RedBall neutron multiplicity meter [12], and several position-sensitive silicon-detector telescopes, respectively.

Figure 1 presents the systematics of multiple IMF emission in the ^{209}Bi + ^{136}Xe reaction at $E/A = 28$ MeV. It is clear from the IMF multiplicity distribution, presented in the top panel (a) of this figure, that in this bombarding-energy domain, multiple IMF emission constitutes an important reaction channel, accounting for a large fraction of the total reaction yield. The plot in Fig. 1(a) includes all events satisfying the "minimum-bias" condition of charged-particle multiplicity $m_c \geq 1$, i.e., includes most of the events.

In Figs. 1(b) and 1(c), the average atomic number $\langle Z_{\mathrm{IMF}} \rangle$ (b) and the average transverse kinetic energy

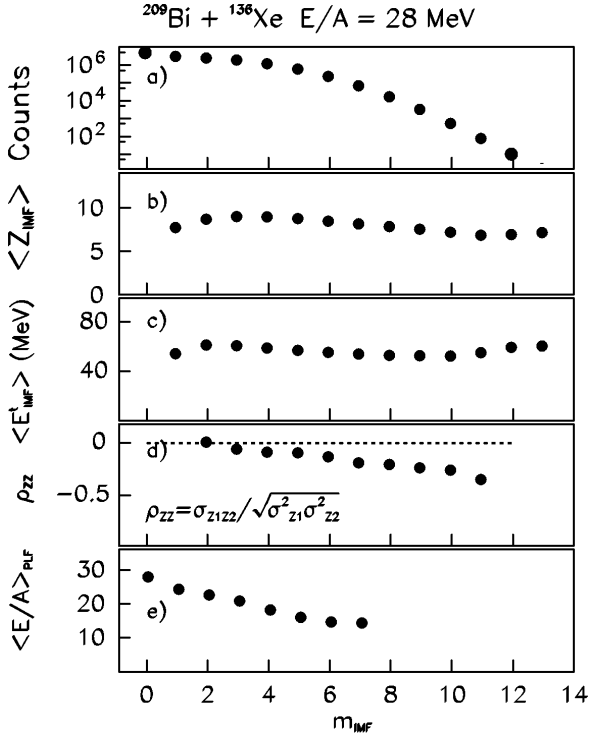

FIG. 1. IMF multiplicity distribution (a) and dependence on the observed IMF multiplicity of average IMF atomic number (b), transverse energy (c), correlation coefficient ρ_{ZZ} (see text) (d), and average PLF kinetic energy per nucleon (in units of MeV) (e).

 0031-9007/96/77(17)/3514(4)$10.00

$\langle E^t_{\rm IMF}\rangle$ (c) of IMFs are plotted as functions of IMF multiplicity $m_{\rm IMF}$. As seen in these panels, both $\langle Z_{\rm IMF}\rangle$ and $\langle E^t_{\rm IMF}\rangle$ are quite large and almost independent of the IMF multiplicity, up to the highest multiplicity of $m_{\rm IMF} = 13$ observed in this reaction. Furthermore, the distributions in $Z_{\rm IMF}$ and $E^t_{\rm IMF}$ are both of exponential character, also largely independent of $m_{\rm IMF}$ [16].

The *independence* of both the $Z_{\rm IMF}$ and $E^t_{\rm IMF}$ distributions of the number of IMFs emitted is the first of the fundamental observations referred to in the introduction. It provides a strong indication for the fact that, in the reaction studied, a single mechanism is primarily responsible for producing these IMFs. This observation suggests also that IMFs are formed almost independently of one another. This latter fact is demonstrated quantitatively in Fig. 1(d), where the correlation coefficient $\rho_{ZZ} = \sigma_{Z1Z2}/(\sigma^2_{Z1}\sigma^2_{Z2})^{1/2}$ is plotted as a function of $m_{\rm IMF}$. This correlation coefficient is defined for a split of the group of IMFs measured in an event into two groups of approximately equal multiplicities which have summed atomic numbers of Z_1 and Z_2, respectively. The quantities σ_{Z1Z2}, σ^2_{Z1}, and σ^2_{Z2} are the covariance and the two variances of the joint distribution of Z_1 and Z_2, respectively. For a scenario in which IMFs acquire their identities independently of each other and at the expense of a large remaining pool of mass and Z, the correlation coefficient would be equal to $\rho_{ZZ} = 0$. With increasing $m_{\rm IMF}$, when the summed charge of all IMFs approaches the total charge of the system, this coefficient would approach $\rho_{ZZ} = -1$, consistent with the trends seen in Fig. 1(d). Similar conclusions regarding the independence of IMF formation were reached by Moretto *et al.* and Phair *et al.* in heavy-ion reaction studies at significantly higher bombarding energies [17].

It has been concluded in earlier works [11,13] that the binary reaction mode accounts for most, if not all, of the total ^{209}Bi + ^{136}Xe reaction cross section at $E/A =$ 28 MeV. A similar conclusion has been reached, e.g., in the studies of ^{197}Au + ^{208}Pb reactions at $E/A = 29$ MeV [18]. The large cross section for IMF production noted above implies then that IMFs are produced and emitted, following a generally binary primary reaction scenario (allowance being made for some pre-equilibrium emission). This is confirmed by the direct observation of fast, projectilelike fragments (PLF) detected at forward angles in coincidence with IMFs. Average kinetic energies per nucleon, $\langle E/A\rangle_{\rm PLF}$, of such PLFs are shown in Fig. 1(e), for events with $m_{\rm IMF} \leq 7$. Here PLF and IMF components in the forward-angle spectra are sufficiently well separated for a reasonably accurate determination of the quantity $\langle E/A\rangle_{\rm PLF}$, where the mass numbers of the PLFs were determined from their measured atomic numbers using a prescription suggested by Charity *et al.* [19]. As seen in Fig. 1(e), the PLFs are slowed down as more and more IMFs are produced, a fact whose significance will become clear further below.

Figure 2 shows Galilei-invariant velocity distributions of protons (left panels) and IMFs with $6 \leq Z_{\rm IMF} \leq 10$ (right panels) associated with $m_{\rm IMF} = 2$ (top panels) and $m_{\rm IMF} = 4$ (bottom panels). The LCP emission patterns in this figure exhibit a superposition of two "Coulomb-Maxwell" ridges characteristic of an emission scenario with two moving sources, as expected for binary processes. In contrast, a similar plot for IMFs features a strong intermediate-velocity component consistent with emission from a neck zone and demonstrates a dynamical IMF production mechanism described earlier [14,20,21]. However, the IMF velocity distributions show also a component with a velocity slightly lower than the PLF velocity that can be associated with nonequilibrium emission from PLFs. One notices that, because of the detection threshold, the corresponding component associated with similar nonequilibrium emission from TLFs would largely be missed by the setup. It will be argued further below, that the above two nonequilibrium components are important for explaining the energy balance in this reaction.

After the observation of an *independence* of the $Z_{\rm IMF}$ and $E^t_{\rm IMF}$ distributions of $m_{\rm IMF}$, discussed previously, the *binary character* of the underlying collision scenario, demonstrated above, constitutes the second fundamental observation referred to in the introduction.

Further key experimental evidence is presented in Fig. 3, where (upper panel) average neutron and light-charged particle (LCP) multiplicities from the ^{209}Bi + ^{136}Xe reaction at $E/A = 28$ MeV are plotted as functions of the associated IMF multiplicity. The effective widths $\Gamma_{\rm FWHM}$ at half-maximum of the respective multiplicity distributions are represented in this figure by vertical bars. The salient feature of the data is a rapid and simultaneous "saturation," with increasing IMF multiplicity of the two observables m_n and $m_{\rm LCP}$. These two observables provide measures of the total intrinsic or

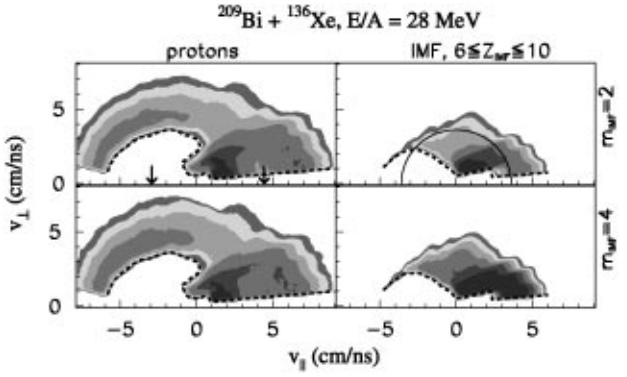

FIG. 2. Galilei-invariant c.m. velocity distributions of protons (left panels) and IMFs with $6 \leq Z_{\rm IMF} \leq 10$ (right panels), for events associated with $m_{\rm IMF} = 2$ (top panels) and $m_{\rm IMF} = 4$ (bottom panels). The arrows indicate projectile and target velocities. A semicircle is drawn to represent an approximate location of the Coulomb-Maxwell ridge for thermal emission from the composite system. The dashed lines indicate the detection thresholds.

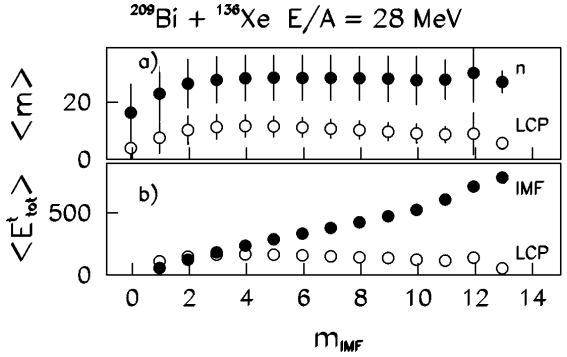

FIG. 3. Average light-particle multiplicities (a), and summed transverse energies (b) (in units of MeV) of IMFs (solid dots) and LCPs (open circles), plotted vs IMF multiplicity. Vertical bars in the upper panel represent the effective widths Γ_{FWHM} of the respective multiplicity distributions.

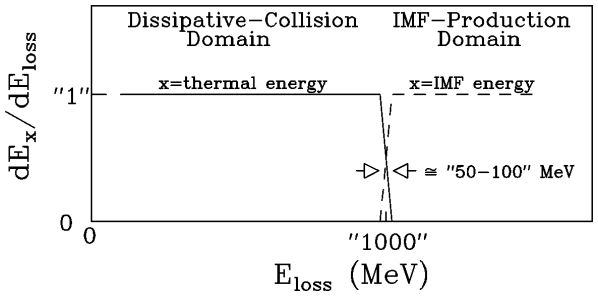

FIG. 4. Pattern of energy conversion from the relative PLF-TLF motion into thermal energy and into IMF degrees of freedom.

thermal excitation of the system, including that of IMFs. A similar saturation is featured by the measured average total transverse energy of LCPs plotted in Fig. 3(b) (open circles) as a function of m_{IMF}. This observation is consistent with earlier reports on incomplete kinetic-energy damping in reactions induced by very heavy ions [11,22]. The light-particle data presented in Figs. 3(a) and 3(b) demonstrate that, as long as the total thermal energy (heat content) of the system is lower than a certain critical value E_c^*, represented by the "saturation" values of m_n and m_{LCP}, the IMF production rate is insignificant. On the other hand, the data also indicate that once the total thermal energy of the system has reached this critical value, no further significant amounts of kinetic energy are converted into heat. The dramatically different trends, illustrated in Fig. 3(b) by the sets of data points for IMFs (solid dots) and LCPs (open circles), the large average values of $\langle E_{\mathrm{IMF}}^t \rangle$, and the large values (tens of MeV [16]) of the logarithmic spectral slopes of the E_{IMF}^t distributions, all prove that the observed IMFs have not competed, to any significant extent, with light particles for the thermal energy deposited in the system. Hence one concludes that IMFs must have been produced dominantly in a dynamical process.

The *saturation* feature of the total thermal excitation energy (heat content) of the system and the *absence of competition* between IMF production and thermal emission processes constitute the third and the fourth fundamental observation, respectively.

The significance of the trends illustrated in Fig. 3 is clarified in Fig. 4, where energy conversion from the relative PLF-TLF motion into other degrees of freedom is pictured schematically. As seen in Fig. 4, up to an energy loss of $E_{\mathrm{loss}} = E_c^*$, virtually all of the "lost" kinetic energy is converted into thermal energy of the system, disregarding any relatively small amounts of deformation energy and of energy carried away by preequilibrium particles. This is the well-known domain of binary dissipative collisions [10,13]. Once the total excitation energy generated in the dissipative stage of the reaction has reached E_c^*, the mechanism of conversion of kinetic energy into heat is rapidly disabled. Instead, a mechanism sets in that converts kinetic energy of collective PLF-TLF motion into potential energy of saddle degrees of freedom and into kinetic energy of individual IMFs. This is a new mechanism of energy dissipation that is not effective at lower thermal excitations of the system. The fact that kinetic energy is expended for IMF production is clear from Fig. 1(d), showing the actual decrease in the PLF velocity as IMFs are formed.

An estimate of the critical excitation energy E_c^* was obtained from statistical-model simulations (code EVAP [23]) by fitting the observed saturation values of m_n and m_{LCP}. Assuming two fragments at equal temperatures and level-density parameters of $a = A/8$, a value of $E_c^* \approx 1$ GeV results, corresponding to a critical temperature of $T_c \approx 5.3$ MeV. One estimates that the width of the transition region between the dissipative and IMF-producing domains is $\Delta E_{\mathrm{loss}} \approx 50{-}100$ MeV. This estimate is derived from a rough assessment of the energy needed to promote one IMF to its saddle configuration and from the observation that "saturation" in m_n and m_{LCP} is reached already at $m_{\mathrm{IMF}} = 2$. The numbers in Fig. 4 are shown in quotation marks in order to emphasize that they are neither very accurate, nor important for the present analysis. What is important is that the transition in the energy conversion pattern is quite rapid on the E_{loss} scale.

There is no completely satisfactory answer to the important question as to what causes such a rapid change in the energy conversion pattern illustrated in Fig. 4. However, the observed, rather sudden disabling of the heat-generation mechanism indicates a substantial change in nuclear response, which may be due to a change in the mean free path of nucleons. The fact that here dynamical IMF production channels open that are closed at lower excitations may indicate changes in mechanical as well as thermal properties of nuclear matter. However, such changes are different from those associated with a liquid-gas transition proposed in the literature. Combined, the new properties of nuclear matter must strongly favor a coupling of the kinetic energy of relative PLF-TLF motion to the saddle configurations of individual IMFs

over the generation of heat. Obviously, these properties also prevent the system from fusing completely.

From considerations of energy balance, one concludes that IMFs are formed of the *moving* PLF and TLF matter, rather than from matter at rest in the center-of-mass frame. This is so because bringing large portions of matter to rest (as is the case for high-m_{IMF} events) would entail the dissipation of large amounts of kinetic energy (of the order of 11 MeV/nucleon). Amounts of heat of the required magnitude are contradicted by the experimental observation of heat deposits limited to approximately 3 MeV/nucleon. One would then expect the IMFs to retain some memory of PLF and/or TLF velocities, consistent with the pattern seen in the bottom right panel of Fig. 2.

In summary, a heavy-ion interaction scenario has been presented which is based on experimental data from the $^{209}\mathrm{Bi} + {}^{136}\mathrm{Xe}$ reaction at $E/A = 28$ MeV, and specifically, on fundamental observations of *independence* of IMF formation, of a *binary character* of the collisions, of a *saturation* of thermal excitation energy, and *of an absence of competition* between IMFs and LCPs for heat energy. This scenario connects, in a natural fashion and within the general binary phenomenology, the domain of dissipative collisions with that of IMF production. Both dissipative collisions and IMF production are driven by the available kinetic energy in the relative PLF-TLF motion. As long as the temperature of the system stays below a certain critical value of $T = T_c$, relative kinetic energy is effectively converted into thermal energy. As the temperature reaches $T = T_c$, a rather rapid change in the kinetic-energy conversion pattern occurs, triggered most likely by a significant change in static or dynamic properties of the matter in the interaction or neck zone. As a result, IMF clusters are formed in this zone at the expense of kinetic PLF-TLF energy, a process which can be viewed as a new mechanism of kinetic-energy dissipation. This IMF clusterization process continues, with decreasing probability, likely until there is no energy or mass left in the binary PLF-TLF degree of freedom. At the end of the interaction, when either all of the kinetic PLF-TLF energy is expended, or when PLF and TLF decouple, the IMF clusters, driven by Coulomb forces, separate from PLFs and TLFs and, after deexcitation, appear as free IMFs.

These findings seriously challenge most models promoted in the literature to describe the multiple-IMF production processes which constitute one of the important reaction modes at intermediate bombarding energies. Clearly, further studies of a variety of interaction systems, and for a range of bombarding energies, have to be conducted in order to establish the systematics of the proposed IMF production mechanism.

This work was supported by the U.S. Department of Energy Grants No. DE-FG02-88ER40414 (University of Rochester), No. DE-FG02-87ER403160, and No. DE-FG02-88ER40406 (Washington University).

*Present address: GANIL (IN2P3-CNRS, DSM-CEA) Caen, France.

[1] C. K. Gelbke and D. H. Boal, Prog. Part. Nucl. Phys. **19**, 33 (1987), and references therein.
[2] B. Borderie *et al.*, Ann. Phys. (Paris) **15**, 287 (1990), and references therein.
[3] D. R. Bowman *et al.*, Phys. Rev. C **46**, 1834 (1992).
[4] L. G. Moretto and G. J. Wozniak, Annu. Rev. Nucl. Part. Sci. **43**, 379 (1993), and references therein.
[5] W. A. Friedman, Phys. Rev. Lett. **60**, 2125 (1988); W. A. Friedman, Phys. Rev. C **42**, 667 (1990).
[6] J. Aichelin, Phys. Rep. **202**, 233 (1991).
[7] D. H. E. Gross, Rep. Prog. Phys. **53**, 605 (1990).
[8] B. Jouault *et al.*, Nucl. Phys. **A597**, 136 (1996).
[9] C. Fauchard and G. Royer, Nucl. Phys. **A598**, 125 (1996).
[10] W. U. Schröder and J. R. Huizenga, in *Treatise in Heavy-Ion Science*, edited by D. A. Bromley (Plenum Press, New York, 1984), Vol. 2, p. 113, and references therein.
[11] B. Lott *et al.*, Phys. Rev. Lett. **68**, 3141 (1992).
[12] S. P. Baldwin, Ph.D. thesis, University of Rochester, Rochester, New York, 1994.
[13] S. P. Baldwin *et al.*, Phys. Rev. Lett. **74**, 1299 (1995).
[14] J. Tõke *et al.*, Phys. Rev. Lett. **75**, 2920 (1995).
[15] D. W. Stracener *et al.*, Nucl. Instrum. Methods Phys. Res., Sect. A **294**, 485 (1990).
[16] J. Tõke *et al.*, Phys. Rev. C (to be published).
[17] L. G. Moretto *et al.*, Phys. Rev. Lett. **74**, 1530 (1995); L. Phair *et al.*, Phys. Rev. Lett. **75**, 213 (1995); L. G. Moretto *et al.*, Phys. Rev. Lett. **76**, 372 (1996).
[18] R. Bougault *et al.*, Nucl. Phys. **A587**, 499 (1995).
[19] R. J. Charity *et al.*, Nucl. Phys. **A476**, 516 (1988).
[20] B. Lott *et al.*, in *Proceedings of the 9th Winter Workshop on Nuclear Dynamics, Key West, 1993* (World Scientific, Singapore, 1993), p. 159.
[21] J. F. Lecolley *et al.*, Phys. Lett. B **354**, 202 (1995); **325**, 317 (1994).
[22] B. M. Quednau *et al.*, Phys. Lett. B **309**, 10 (1993).
[23] N. Nicolis *et al.*, computer code EVAP (unpublished); evolved from code PACE by A. Gavron, Phys. Rev. C **21**, 230 (1980).